The Journal of Immunology

Reactivation of Neutralized HIV-1 by Dendritic Cells Is Dependent on the Epitope Bound by the Antibody

Thijs van Montfort, Adri A. M. Thomas, Przemek M. Krawczyk, Ben Berkhout, Rogier W. Sanders and William A. Paxton

J Immunol 2015; 195:3759-3768; Prepublished online 9 September 2015;
doi: 10.4049/jimmunol.1402344
http://www.jimmunol.org/content/195/8/3759

The Journal of Immunology is published twice each month by
The American Association of Immunologists, Inc.,
9650 Rockville Pike, Bethesda, MD 20814-3994.

Print ISSN: 0022-1767 Online ISSN: 1550-6606.

Reactivation of Neutralized HIV-1 by Dendritic Cells Is Dependent on the Epitope Bound by the Antibody

Thijs van Montfort,* Adri A. M. Thomas,† Przemek M. Krawczyk,‡ Ben Berkhout,* Rogier W. Sanders,*,§ and William A. Paxton*,¶

Ab-neutralized HIV-1 can be captured by dendritic cells (DCs), which subsequently transfer infectious HIV-1 to susceptible CD4$^+$ T cells. In this study, we examined the capacity of early Abs, as well as recently identified broadly neutralizing Abs (bNAbs) targeting different envelope glycoprotein (Env) epitopes, to block HIV-1 transmission by immature and mature DCs to HIV-1–sensitive cells. Three bNAbs directed against the gp41 membrane proximal region of Env (2F5, 4E10, and 10E8) and three gp120 bNAbs targeting the CD4 binding site (b12, VRC01, and NIH45-46) were examined. In addition, eight glycan-dependent bNAbs targeting the V1V2 apex (PG9, PG16, and PGT145), the V3 loop (2G12, PGT121, and PGT128), and the gp120–gp41 interface of Env (PGT151 and 35O22) were tested. bNAbs that bound specific glycans showed, depending on the immature or mature state of the DC, diverse efficiencies in HIV-1 *trans*-infection. All bNAbs that bound the CD4 binding site blocked *trans*-infection, whereas all bNAbs directed against the membrane proximal region lost neutralizing activity after DC-mediated HIV-1 transmission. To understand how preneutralized HIV-1 can be transferred as infectious virus by DCs, we followed the processing of 2F5-treated HIV-1 by DCs with confocal microscopy. Inhibition of DC-internalization pathways could not reverse the dissociation of 2F5 from HIV-1, suggesting that Ab dissociation occurs directly at the plasma membrane. Collectively, these findings imply that the location of the epitope and the neutralization capacity of these Abs determine the efficiency of DC-mediated HIV-1 transfer. *The Journal of Immunology*, 2015, 195: 3759–3768.

Dendritic cells (DCs) reside within the skin and mucosal epithelia in an immature state (1, 2). Nonself-antigens are captured with an array of specific surface molecules designated as pattern recognition receptors (3–5). DC-entrapped Ags are processed into small peptides to enhance innate and adaptive immune responses (6, 7).

DCs were shown to transfer HIV-1 toward susceptible target CD4$^+$ T lymphocytes in *cis* and in *trans* (8). HIV-1 transmission in *cis* is characterized by direct infection of the DC, which takes a few days, resulting in transfer of de novo–produced virions (9, 10). DC-mediated HIV-1 transmission in *trans* relies on the capture of HIV-1 particles, followed by transfer to HIV-1–susceptible CD4 cells. Typically, *trans*-infection starts within a few hours following capture and can continue for a few days (9, 11). Transmission of HIV-1 from DCs to CD4$^+$ T lymphocytes occurs via formation of a virological synapse upon cell–cell contact (12–15). Cavrois et al. (9) showed that membrane-bound HIV-1 was transmitted to susceptible cells, whereas internalized HIV-1 was degraded. Other studies reported that LPS-matured DCs recruited captured HIV-1 into deep, invaginated membrane pockets, where the virus is redirected to the virological synapse to be transmitted to HIV-1 susceptible cells (11, 16–19).

Capture of HIV-1 by immature DCs (iDCs) relies on high-affinity oligo-mannose glycans on the HIV-1 envelope glycoprotein (Env) that interact with C-type lectins, like DC-SIGN, and proteoglycans (20), such as syndecan 1-4 (21, 22). In contrast, LPS-matured DCs (mDCs) capture HIV-1 predominantly with Siglec-1/CD169, which interacts with sialyllactose-containing gangliosides embedded in the membrane of the virion (23–25). iDCs can also capture HIV-1 via Siglec-1; however, because of the lower expression of this receptor and the higher expression of C-type lectin receptors, such as DC-SIGN, virus capture is primarily Env dependent.

We demonstrated previously that neutralized HIV-1 captured by DCs could regain infectivity upon viral transmission in *trans* to CD4$^+$ T lymphocytes (26, 27). Most Abs, such as 2F5, 4E10, or V3, could not prevent this DC-mediated viral transmission; in contrast, the b12 Ab efficiently blocked viral transfer. The reason why b12 behaved differently is unknown and is part of this study. Recently, some new extremely potent broadly neutralizing Abs (bNAbs) were described. In this study, we determined the DC-mediated transfer of HIV-1, neutralized with each of these bNAbs, and compared the effect of these Abs with some well-described bNAbs. Three membrane proximal region (MPER)-directed bNAbs (2F5, 4E10 and 10E8), three CD4 binding site bNAbs (b12, VRC01 and NIH45-46), and eight glycan-dependent bNAbs targeting V1V2-glycans (PG9, PG16, and PGT145), outer domain glycans (2G12, PGT121, PGT128), and gp120–gp41

*Laboratory of Experimental Virology, Department of Medical Microbiology, Center for Infection and Immunity Amsterdam, Academic Medical Center of the University of Amsterdam, 1105 AZ Amsterdam, the Netherlands; †Developmental Biology, Department of Biology, Faculty Betascience, University Utrecht, 3584 CH Utrecht, the Netherlands; ‡Department of Cell Biology and Histology, Academic Medical Centre of the University of Amsterdam, 1105 AZ Amsterdam, the Netherlands; §Department of Microbiology and Immunology, Weill Medical College of Cornell University, New York, NY 10065; and ¶Clinical Infection, Microbiology, and Immunology, Institute of Infection and Global Health, University of Liverpool, Liverpool L69 7BE, United Kingdom

Received for publication September 16, 2014. Accepted for publication August 3, 2015.

Address correspondence and reprint requests to Dr. Thijs van Montfort, Laboratory of Experimental Virology, Department of Medical Microbiology, Center for Infection and Immunity Amsterdam, Academic Medical Center of the University of Amsterdam, Meibergdreef 15, 1105 AZ Amsterdam, the Netherlands. E-mail address: t.vanmontfort@amc.uva.nl

Abbreviations used in this article: bNAb, broadly neutralizing Ab; DC, dendritic cell; DT_{50}, 50% degradation time; Env, envelope glycoprotein; $HIV\text{-}1_{GFP}$, GFP-fluorescent HIV-1; IC, immune complex; iDC, immature DC; iMDDC, immature monocyte-derived DC; mDC, LPS-matured DC; mMDDC, mature monocyte-derived DC; MPER, membrane proximal region; NIH, National Institutes of Health; PNGS, potential *N*-linked glycan site.

www.jimmunol.org/cgi/doi/10.4049/jimmunol.1402344

interface glycans (PGT151 and 35O22) were tested. All MPER bNAbs could not neutralize HIV-1 after DC-mediated transmission *in trans*, whereas all CD4bs bNAbs efficiently blocked HIV-1 transfer from DCs. To characterize the observed difference between CD4bs and MPER bNAbs, we followed the processing of 2F5- and b12-neutralized HIV-1 in iDCs and mDCs. During internalization, the 2F5 bNAb readily dissociated from HIV-1, whereas the b12 bNAb remained firmly bound. No specific internal compartment of the endocytic pathway could be identified as being responsible for the dissociation of 2F5 from the virus. Rather, Ab dissociation occurred on the plasma membrane directly after capture of the HIV-1–Ab complex.

Materials and Methods

Abs and reagents

All bNAbs were used at 20 μg/ml, or as indicated in the figure legends, and were obtained as gifts or purchased from the following sources: John Mascola and Peter Kwong (VRC01); Dennis Burton and P. Parren (b12, PG9, PG16, PGT121, PGT128, and PGT145); Polymun Scientific (2F5, 4E10, and 2G12); Michel Nussenzweig (NIH45-46); and National Institutes of Health (NIH) AIDS reagent program (10E8 H and L chain). IgG1 obtained from a patient with a B cell lymphoma was used as a nonspecific control Ab; the sera contained IgG1-λ M protein (83 mg/ml) and no detectable IgA or IgM (<0.06 mg/ml). mAbs to stain DC compartments, CD81, DC-SIGN, EEA1, HLA-DR, CD63, HLA-DM, and LAMP-1, were obtained from BD Pharmingen. Secondary Abs, AffiniPure donkey anti-human–Cy3 and donkey anti-mouse–Cy5, were acquired from Jackson ImmunoResearch Laboratories and used at a 50-fold and 200-fold dilution, respectively. Nuclear DNA was stained with Hoechst 33258.

Cells

The HIV-1–permissive CD4, CCR5, and CXCR4–expressing TZM-bl reporter cell line (NIH AIDS reagent program), containing luciferase and β-galactosidase genes under the control of the HIV-1 long terminal repeat promoter, was cultured and maintained in DMEM (Invitrogen, Breda, the Netherlands) containing 10% FCS (HyClone, Perbio, Etten-Leur, the Netherlands), MEM nonessential amino acids (0.1 mM; Invitrogen), and penicillin/streptomycin (both at 100 U/ml). HEK 293T cells were cultured and maintained in DMEM containing 10% FCS. Immature monocyte-derived DCs (iMDDCs) were prepared as previously described (26). In short, human blood monocytes were isolated from buffy coats using a Ficoll gradient and a subsequent CD14 selection step using a magnetic bead cell sorting system (Miltenyi Biotec, Bergisch Gladbach, Germany). Purified monocytes were differentiated into iMDDCs by treatment with 45 ng/ml IL-4 (BioSource) and 500 U/ml GM-CSF (Schering-Plough, Brussels, Belgium) on days 0 and 3. Cells were used on day 6. Mature monocyte-derived DCs (mMDDCs) were obtained on day 6 after stimulating iMDDCs on day 5 with 20 μg polyinosinic-polycytidylic acid/ml (Sigma-Aldrich, St. Louis, MO). The phenotypes of both types of DCs were confirmed by flow cytometry (27).

Virus production

Molecular cloned R5X4 GFP-fluorescent HIV-1 (26, 27) was generated by cotransfecting HEK 293T cells with GFP-VPR and full-length proviral 299.10ΔgV3 HIV-1 vector (28) in a 1:1 ratio. The supernatant, containing HIV-1_{GFP}, was collected 3 d after transfection and concentrated using Amicon Ultra filters (100,000 m.w. cut-off). The concentration of viral capsid (CA-p24) was determined by ELISA. GFP-fluorescent HIV-1 (HIV-1_{GFP}) was frozen in small aliquots. The BG505 HIV-1 strain was constructed by cotransfecting HEK 293T cells in a 1.5:1 ratio with Env encoding BG505.T332N plasmid and the HIV-1 proviral backbone pSG3ΔEnv (from Drs. John C. Kappes and Xiaoyun Wu, AIDS Research and Reference Reagent Program, Division of AIDS, National Institute of Allergy and Infectious Diseases, NIH).

DC-mediated virus transmission to TZM-bl cells

HIV-1 (30 ng/ml CA-p24) was treated with various concentrations of control IgG1 or bNAbs for 1 h. Subsequently, Ab-treated HIV-1 was added to iMDDCs or mMDDCs for 2 h. Unbound virus and bNAb was removed by washing the cells three times with RPMI 1640 medium supplemented with 10% FCS. DCs were cocultured with TZM-bl reporter cells for 48 h in the presence of 400 nM saquinavir (Roche, Basel, Switzerland) to prevent virus maturation. HIV-1 infection of the reporter cells was quantified by measuring luciferase activity.

Virus infectivity

TZM-bl cells were cultured to 70–80% confluence in 96-well plates. Cells were washed once with PBS before adding free virus supernatant (5 ng/ml CA-p24) or 1.0×10^5 DCs loaded with virus, in the presence of 400 nM saquinavir, a protease that prevents synthesis of new infectious virions (Roche), and 40 μg/ml DEAE-dextran (Sigma-Aldrich) in a total volume of 200 μl. Medium was removed 2 d postinfection, and the cells were washed once with PBS before lysis with Reporter Lysis Buffer (Promega, Madison, WI). Luciferase activity was measured using a Luciferase Assay kit (Promega) and a GloMax luminometer, according to the manufacturer's instructions (Turner BioSystems, Sunnyvale, CA). All infections were performed in triplicate. Background luciferase activity, as determined using uninfected cells, was subtracted from experimental values.

Virus capture and localization

HIV-1_{GFP} was incubated with 20 μg/ml control human IgG1 or 2F5 or b12 Ab for 45 min. To follow the localization of the Ab, secondary anti-human Cy3 Ab was added for 15 min. iMDDCs or mMDDCs were inoculated for 2 h with the HIV-1–Ab mixture at 37˚C. Unbound virus and Ab were removed by washing three times with PBS, and cells were seeded on pretreated poly-L-lysine–coated coverslips (1 mg/ml). Within 5 min, cells were fixed in 3.7% paraformaldehyde for 20 min. Paraformaldehyde was quenched with 50 mM NH_4Cl, and cells were permeabilized with 0.1% saponin (Sigma-Aldrich), 10 mM NH_4Cl, and 1% BSA in PBS for 30 min. Subsequently, cells were stained with primary mouse Ab CD81, DC-SIGN, EEA1, HLA-DR, CD63, HLA-DM, or LAMP-1 and Cy5-coupled donkey anti-mouse secondary Ab; nuclear DNA was stained with Hoechst 33258. Excess Ab was removed by washing twice with permeabilization buffer, once with PBS, and twice with water. Cells were embedded in VECTASHIELD, and fluorescence was analyzed by confocal microscopy. HEK 293T cells were transiently transfected with plasmid DNA encoding human FcγRI, and expression was observed 24 h later (data not shown). Cells were incubated for 2 h with HIV-1 pretreated with 20 μg/ml control human IgG1 or 2F5 or b12 Ab at 37˚C. Cells were collected, and unbound virus was removed by washing three times with PBS. Cells were lysed with 1% EMPIGEN, and CA-p24 was determined using standard ELISA.

Virus degradation

iMDDCs or mMDDCs (5.0×10^4 cells/well in 100 μl) were seeded in a flat-bottom 96-well plate and mixed with HIV-1 (5 ng CA-p24/well in 100 μl) that was preincubated or not with 20 μg/ml 2F5 or b12 Ab for 1 h. HIV-1 was incubated with the cells for the time indicated at 37˚C before cells were lysed with 50 μl 1% EMPIGEN. Degradation of virus was determined by measuring the remaining CA-p24 using standard ELISA.

Confocal analyses

Fluorescent images were taken using a Leica DM SP2 AOBS confocal microscope with a ×63 HCX PL APO 1.32 oil-immersion objective. A cell was scanned in 20 images (512 × 512), with a pixel size of 232 nm and a step size of 340 nm, and analyzed with the Leica confocal imaging processing software with a line average of two scans/image. The number of HIV-1_{GFP} spots was counted for each cell. Colocalization was analyzed using a semiautomatic program based on DIPimage (TU Delft, the Netherlands), custom-written in Matlab. Briefly, the threshold for the different image channels was determined using the Isodata algorithm, and colocalization was determined on overlapping pixels from images taken per frame (z-stack)/cell.

Statistical analysis

Significance was determined with the unpaired *t* test (two tailed).

Results

The efficiency of HIV-1 neutralization by bNAbs upon DC transmission depends on the Env epitope bound by the Ab

We previously determined that neutralizing Abs could not prevent *trans*-infection when iMDDCs, inoculated with neutralized HIV-1, were incubated with $CD4^+$ T cells. Of a panel of different bNAbs, only the CD4bs Ab b12 was able to prevent DC-mediated *trans*-infection, whereas two Abs directed to MPER of gp41, 2F5 and 4E10, could not (26). To determine whether the efficiency of Ab neutralization following *trans*-infection by DCs is dependent on Ab potency or specificity for Env epitope binding sites, we tested

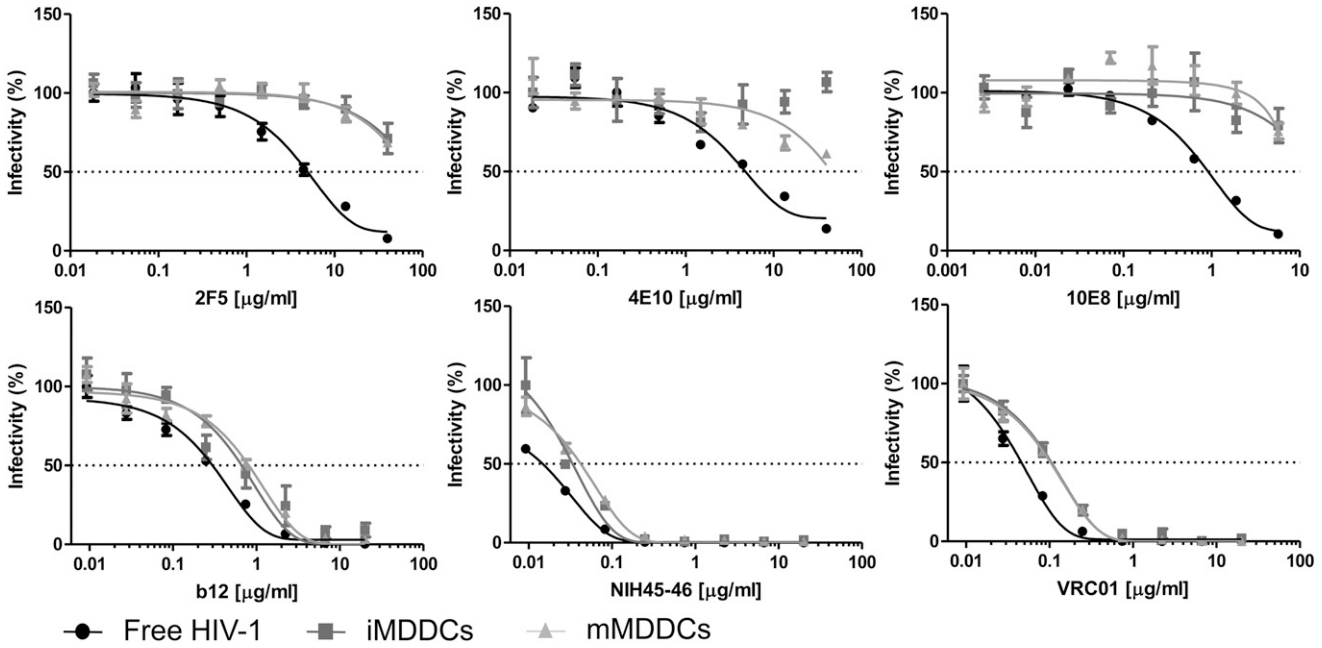

FIGURE 1. *Trans*-infection efficiency of HIV-1 neutralized by MPER or CD4bs bNAbs. HIV-1 was neutralized with different concentrations of various bNAbs, and infection efficiency of cell-free virus or viral transfer by iMDDCs and mMDDCs was measured. Three MPER-binding bNAbs (2F5, 4E10, and 10E8) and three CD4bs Abs (b12, 45-46, and VRC01) were tested in quadruplicate.

newly identified MPER bNAb 10E8, as well as two highly neutralizing CD4bs Abs, NIH45-46 and VRC01 (Fig. 1). All three MPER-directed bNAbs blocked infection of free virus, but marginally blocked HIV-1 transmission by iMDDCs or mMDDCs. In contrast, all CD4bs bNAbs tested efficiently blocked HIV-1 infection, as well as DC-mediated HIV-1 transmission. Neutralization of DC-transmitted virus by CD4bs Abs was ~2.5–3.5-fold less efficient than was neutralization in the absence of DCs (Table I). These results indicate that neutralization after transmission is related to specificity of the Abs and not on their neutralization titer.

Glycan-dependent bNAbs have diverse effects on DC-mediated HIV-1 transmission

To investigate whether the different bNAbs have a specific profile in DC-mediated HIV-1 transmission, we tested a panel of newly identified glycan-dependent bNAbs. Potential *N*-linked glycan sites (PNGS) that are required for these bNAbs were present in the R5X4 virus (156, 160, 230, 241, 295, 301, 332, 339, 386, 392, 611, 625, 637, according to LAI numbering) (Table I). The PG9, PG16, and PGT145 bNAbs that bind the N156 and N160 glycan on the apex of the Env trimer neutralized free HIV-1 only weakly at the highest concentration (Fig. 2A). PG9 was able to block iMDDC-mediated HIV-1 *trans*-infection by 60% at 1 μg/ml; no inhibition was observed with mMDDCs. PG16 and PGT145 did not block *trans*-infection mediated by iMDDCs, but a remarkable 2–4-fold enhanced transmission was observed with mMDDCs. The glycan-dependent bNAbs 2G12, PGT121, and PGT128, which all require the N332 glycan that is the center of the outer domain oligomannose patch (29), in addition to diverse neighboring glycans, neutralized free virus moderately. However, these bNAbs blocked HIV-1 *trans*-infection more efficiently when transferred by iMDDCs compared with neutralization of free virus, but

Table I. Neutralization of bNAbs of R5X4 HIV-1 with and without DCs

bNAbs Binding Env from Top to Bottom		Glycans Present on the R5X4 Virus That Can Mediate Binding		50% Neutralization (IC_{50}; μg/ml)		
bNAb	Epitope	Glycan Position	Refs.	Free HIV-1	iMDDC	mMDDC
PG9	V1V2	N156/N160	(30, 31, 46)	10	0.2	NN
PG16	V1V2	N156/N160	(31, 46, 47)	>20	NN	NN↑
PGT145	V1V2, quaternary	N160		>20	NN	NN↑
2G12	Outer domain	N295/**N332**/N339/N386/N392	(48, 49)	0.15	3.3	>40
PGT121	V3	N301/**N332**	(50–52)	1.1	0.12	0.32
PGT128	V3	N295/N301/**N332**	(51, 53, 54)	NN	1	NN↑
PGT151	gp41–gp120 interface, quaternary	N611/N637	(55, 56)	0.02	0.08	0.02
35022	gp41–gp120 interface, quaternary	N88/N230/N241/N625	(57, 58)	>20	NN	NN
b12	CD4bs	NA		0.3	0.7	0.8
NIH45-46	CD4bs	NA		0.02	0.03	0.04
VRCO1	CD4bs	NA		0.05	0.1	0.1
2F5	MPER	NA		4.5	>40	>40
4E10	MPER	NA		4.8	NN	>40
10E8	MPER	NA		9.0	>40	>40

Infectivity of R5X4 HIV-1 was determined with different bNAbs, with or without iMDDCs and mMDDCs. The 50% neutralization titer is given (IC_{50}). Partial neutralization that did not reach 50% neutralization is indicated by > with the highest used Ab concentration.

The position, according to HXB2 amino acid numbering, is given. The N332 PNGS is in bold type.

NA, not applicable; NN, no neutralization; NN↑, enhanced infectivity

they were less or not effective in blocking HIV-1 *trans*-infection by mMDDCs, and PGT128-treated HIV-1 enhanced *trans*-infection at high concentrations. The glycan-dependent gp120–gp41 interface bNAb PGT151 neutralized free HIV-1 efficiently, and transmission via DCs was similarly hampered. In contrast, 35O22, which binds to a different glycan-dependent epitope at the gp120–gp41 inter-

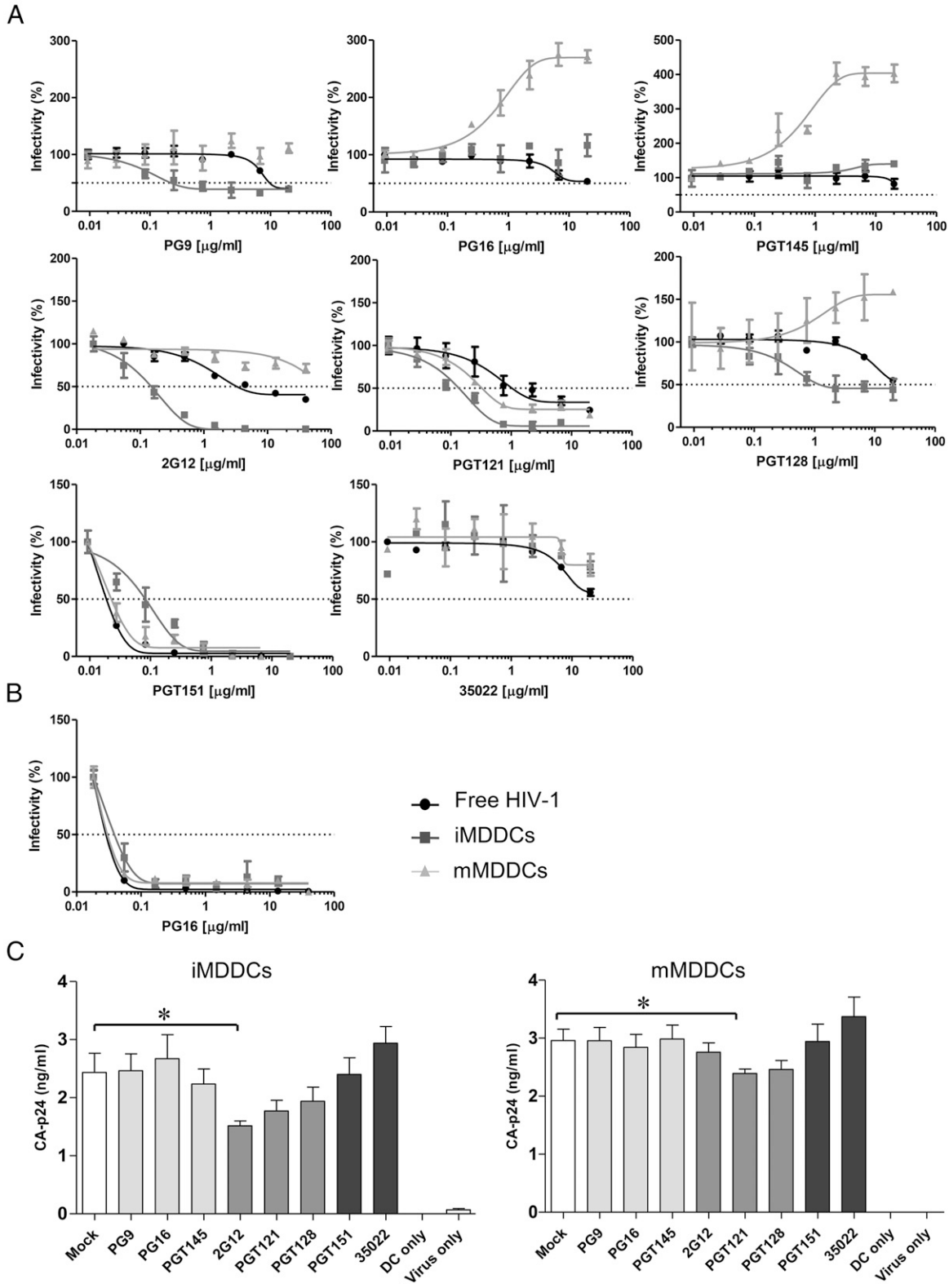

FIGURE 2. *Trans*-infection efficiency of HIV-1 neutralized by glycan-dependent bNAbs. (**A**) HIV-1 was neutralized with different concentrations of various bNAbs, and infection efficiency of cell-free virus or viral transfer by iMDDCs and mMDDCs was measured. Six glycan-dependent bNAbs (2G12, PG9, PG16, PGT121, PGT128, and PGT145) were tested in quadruplicate. (**B**) Env pseudotyped BG505 HIV-1 was neutralized with different concentrations of PG16, and infection efficiency of cell-free virus or viral transfer by iMDDCs and mMDDCs was measured in quadruplicate. (**C**) Capture of mock or bNAb-treated HIV-1 by iMDDCs or mMDDCs. *$p \leq 0.05$.

face, did not block free virus or affect the *trans*-infection efficiency mediated by DCs, despite the presence of all required glycans in the R5X4 virus used for this study.

Because PG16 clearly enhanced transfer of the R5X4 strain and, thus, bound this virus, we repeated the *trans*-infection experiment with HIV-1 BG505, a strain with an identical PNGS pattern, but with a lysine at position 169 in β-strand C in the V1V2 instead of glycine. This lysine is essential for neutralization by this bNAb (30, 31). Free BG505 virus, as well as DC-transmitted BG505, was neutralized efficiently at a very low PG16 concentration (IC_{50} ~ 0.03–0.04 μg/ml) (Fig. 2B). The results for PG16 obtained with the R5X4 strain (Fig. 2A) and BG505 (Fig. 2B) suggest that, for this bNAb, a single amino acid change within the epitope can decrease neutralization and even favor viral dissemination by mMDDCs.

Next, we assessed the effect of the different glycan-dependent bNAbs on HIV-1 capture by iMDDCs and mMDDCs. The three bNAbs that target the N332 glycan in the outer domain oligomannose patch, 2G12, PGT121, and PGT128, diminished HIV-1 capture by iMDDCs, whereas the other glycan-dependent bNAbs showed no effect (Fig. 2C). For, mMDDCs, PGT121 reduced virus capture marginally. In summary, glycan-dependent bNAbs can either decrease or increase the DC-mediated HIV-1 *trans*-infection efficiency, which is dependent on the neutralizing capacity of the Abs and processing of the Ab–HIV-1 complex by DCs.

Processing of neutralized HIV-1–Ab complexes by DCs is Ab dependent

It appears that all MPER-directed bNAbs could not neutralize HIV-1 transferred by DCs, whereas all CD4bs could. To investigate how preneutralized HIV-1 can be transferred as infectious virus, we followed the HIV-1–Ab complexes by confocal microscopy. HIV-1_{GFP} was mixed with a high concentration of fluorescently labeled 2F5, b12, or control IgG1, and processing of HIV-1 and Abs in immune complexes (ICs) by iMDDCs and mMDDCs was visualized (Fig. 3). Little colocalization between 2F5 or control IgG1 and HIV-1_{GFP} was observed for iMDDCs (Fig. 3A) and mMDDCs (Fig. 3B). In contrast, the b12 bNAb colocalized strongly with HIV-1_{GFP} for both DC types. These results show that

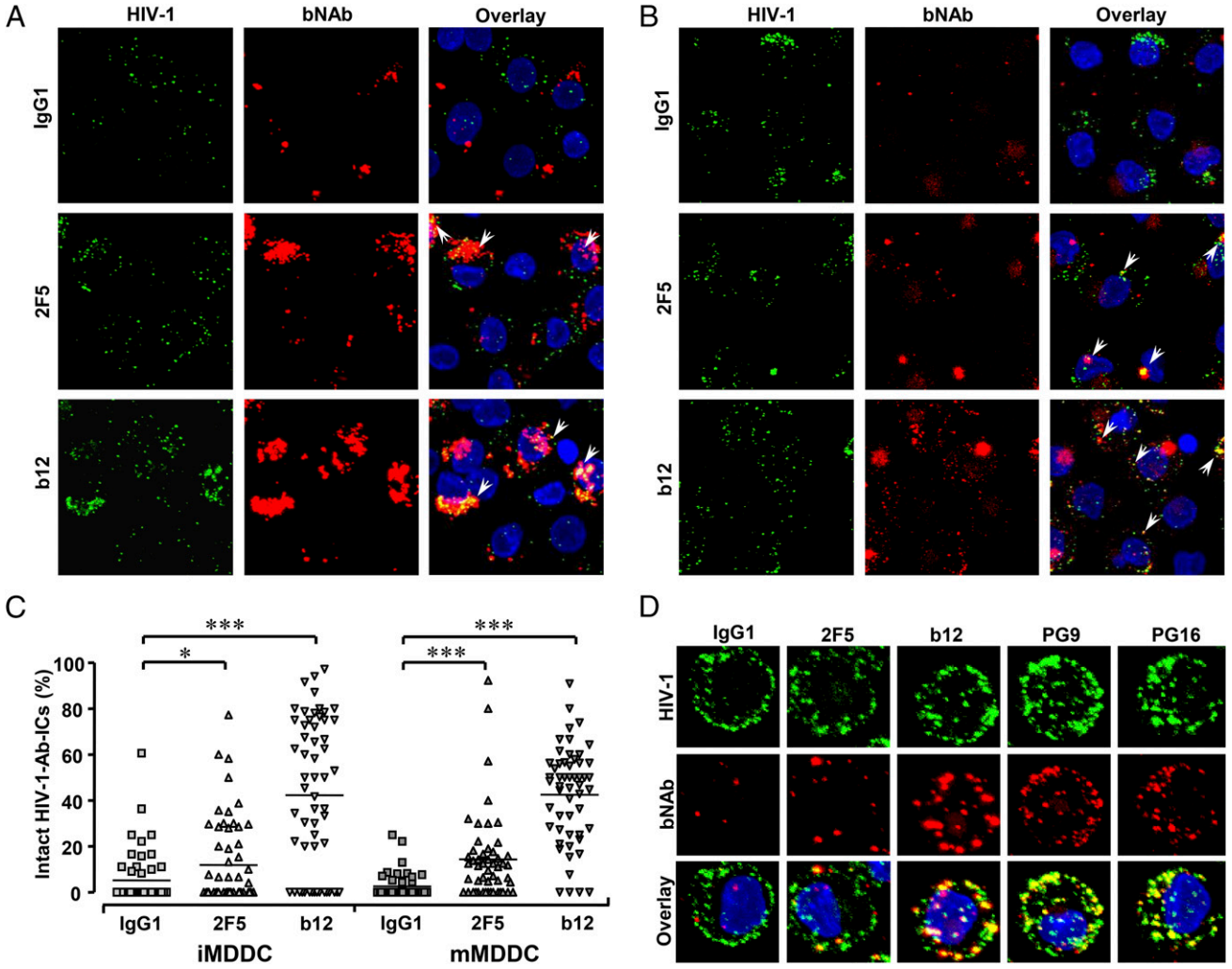

FIGURE 3. HIV-1–Ab complexes captured by DCs. HIV-1_{GFP} particles were treated with 2F5, b12, or control IgG1-labeled Ab and captured by iMDDCs (**A**) or mMDDCs (**B**) for 2 h. Small or big HIV-1 clusters colocalized with bNab are pointed out by white arrowheads. HIV-1 virions (green; *left panels*), Abs (*middle panels*), and nuclear DNA (blue) were detected by confocal microscopy. HIV-1–Ab complexes were visualized by colocalization of HIV-1 and Ab signal and plotted as overlay in yellow (*right panels*). (**C**) The– number of HIV-1 colocalized with bNAb was determined as the number of overlapping green and red pixels as the percentage of green pixels/single cell. Data are mean ± SEM from >50 cells. (**D**) Colocalization of HIV-1 (green) and indicated bNAb (red) captured by mMDDCs. Nuclear DNA is shown in blue. Cells in (A), (B), and (D) were magnified with a ×64 objective and scanned with a 2× zoom. $*p \leq 0.05$, $***p \leq 0.0005$.

2F5 easily dissociates from HIV-1 and explain why 2F5-treated HIV-1 is transmitted as an infectious virus by iMDDCs or mMDDCs (Fig. 2A), whereas b12-treated HIV-1 remains neutralized when transmitted and is unable to infect HIV-1–susceptible cells. Remarkably, not all b12-treated HIV-1_{GFP} captured by iMDDCs or mMDDCs colocalized with the bNAb. This may explain, in part, why the neutralization titer of CD4bs bNAbs after transmission by DCs is slightly higher than for free HIV-1 (Fig. 1).

The percentage of intact HIV-1–bNAbs ICs captured by DCs was determined by measuring the number of overlapping Ab and GFP pixels as the percentage of total GFP pixels. For 2F5, the percentage was 11.9% for iMDDCs and 14.4% for mMDDCs (Fig. 3C). In contrast, the percentage of intact HIV-1–b12 Abs ICs for iMDDCs and mMDDCs was 42.3 and 42.6%, respectively. Control IgG1-treated HIV-1_{GFP} gave background binding of 5.2% for iMDDCs and 2.6% for mMDDCs. These data illustrate that HIV-1– b12 Ab ICs are more resistant to DC-mediated Ab dissociation than are HIV-1 ICs formed with 2F5.

To determine whether glycan-dependent bNAbs, which weakly neutralized the R5X4 strain (Fig. 2A), could bind the virus used, we visualized colocalization of captured HIV-1_{GFP} by mMDDCs with PG9 and PG16 (Fig. 3D). As control, colocalization of HIV-1_{GFP} with 2F5, b12, and irrelevant IgG1 was examined. Like b12, both PG9 and PG16 colocalized with HIV-1_{GFP}, whereas 2F5 and control IgG1 did not. Thus, although bNAbs can bind HIV-1 (Fig. 3D), they do not necessarily neutralize (Fig. 2A).

HIV-1 complexed with 2F5 is degraded as efficiently as untreated virus

Captured Ab ICs can be retained for prolonged periods in DCs, allowing longer presentation of peptides (32). To measure the stability of the HIV-1–Ab IC, viral degradation was determined in iMDDCs and mMDDCs by measuring CA-p24. Decay of HIV-1 in the presence of either control IgG1 or 2F5 after capture by iMDDCs was similar, with a 50% degradation time (DT_{50}) ~ 90 min (Fig. 4). HIV-1 preneutralized with b12 was slightly more stable in iMDDCs, with a DT_{50} of 200 min. HIV-1 was considerably more stable in polyinosinic-polycytidylic acid–matured DCs, with a DT_{50} ~ 1000 min for Ab-treated and untreated HIV-1. Even after 72 h, 30% of input CA-p24 could still be measured, suggesting that HIV-1 was still intact and could be transferred to susceptible cells. Collectively, these results show that HIV-1–b12 ICs are ~2-fold more stable than HIV-1–2F5 ICs in iMDDCs and that iMDDCs and mMDDCs process HIV-1 at a different rate.

Dissociation of 2F5 from HIV-1 does not occur in a compartment of the endocytic pathway

Given that 2F5 binding to virus particles is lost during DC processing, we examined in which cellular compartment this might occur. Plasma membrane (CD81, DC-SIGN, MHC class II [in mDCs]), early endosomes (EEA1), multivesicular bodies (CD63, HLA-DM, MHC class II [in iDCs]), and lysosomes (LAMP-1) were stained to visualize in which of these compartments 2F5–HIV-1 ICs dissociated. Representative photomicrographs of fluorescent 2F5–HIV-1 ICs processed by iMDDCs and mMDDCs are shown in Fig. 5A and 5B. Localization of HIV-1 and 2F5 was analyzed in the different compartments in both DC types (Fig. 5C, 5D). We did not observe differences in the distribution of HIV-1 particles clustering with 2F5 Ab (Fig. 5C, 5D, *left panels*) or not clustering with 2F5 Ab (Fig. 5C, 5D, *right panels*). HIV-1 captured by iMDDCs clustered most strongly with the plasma membrane marker CD81 (~28–33%) and DC-SIGN (~35–45%) (Fig. 5C). These results suggest that the remaining 60% of HIV-1 particles should be localized with intracellular markers. However,

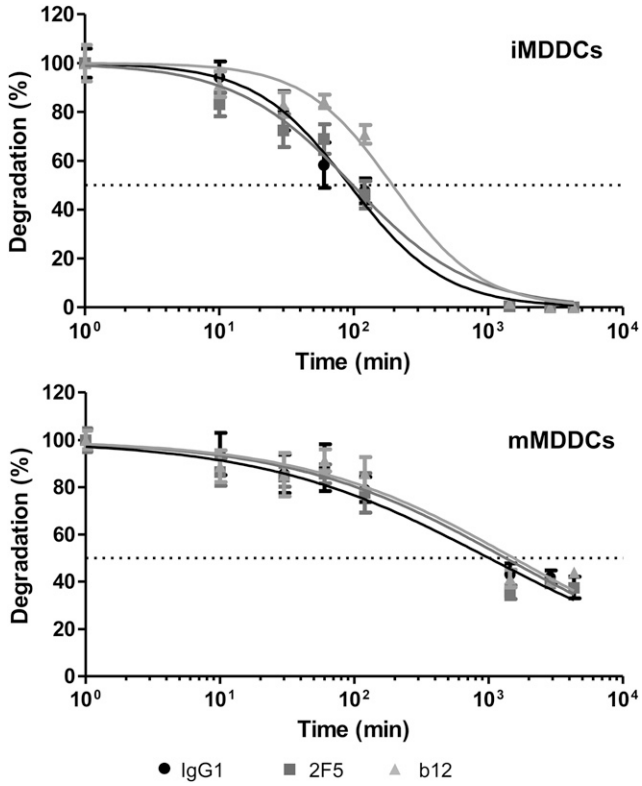

FIGURE 4. Virus degradation by DCs. Degradation of HIV-1 pretreated with bNAb 2F5 or b12 by iMDDCs or mMDDCs was determined by measuring detectable viral CA-p24 as the percentage of input CA-p24.

only 35% of HIV-1 particles colocalized with endosomal pathway markers (EEA1 ~8%, MHC class II ~9%, CD63 ~8%, HLA-DM ~6%, and LAMP-1 ~4%). The low level of intact HIV-1 virions in LAMP-1^+ lysosomes is likely due to protein degradation and loss of the GFP signal in this compartment. Colocalization in mMDDCs of 2F5–HIV-1 ICs or uncomplexed HIV-1 showed a higher percentage of virus at the plasma membrane (CD81 ~63%, DC-SIGN ~52%, and MHC class II ~34%) (Fig. 5D). The increase in HIV-1 colocalization with MHC class II on mMDDCs probably resulted from recruitment of MHC class II to the plasma membrane upon DC maturation (27). Coinciding with a high level of HIV-1 at the plasma membrane of mMDDCs, we observed a reduction in virus colocalized with a number of intracellular markers (EEA1 ~3%, CD63 ~5%, and HLA-DM ~4%). The results indicate that the majority of reactivation of HIV-1 likely occurs at the plasma membrane and not in intracellular vesicles.

HIV-1–2F5 Ab dissociation occurs at the plasma membrane

To further assess the location where HIV-1 dissociates from 2F5, we blocked internalization at various stages. Macropinocytosis and phagocytosis was blocked with cytochalasin D, latrunculin, or wortmannin. Lipid raft and caveolae-mediated endocytosis was blocked with filipin, and clathrin-mediated endocytosis was blocked with monodansylcadaverine (33). Pinching of endocytic vesicles from the plasma membrane was blocked with dynasore. Nocodazole was used to inhibit intracellular microtubule-dependent transport activity. Drug concentrations were used that are effective at blocking a particular internalization pathway, as described in the literature. None of the tested drugs inhibited dissociation of 2F5 from HIV-1; treatment with cytochalasin D and latrunculin even increased dissociation of HIV-1 from 2F5 (Fig. 6A, 6B). Treatment of mMDDCs with a combination of cytochalasin D, filipin, and monodansylcadaverine or a change in

temperature to 4˚ or 16˚C did not alter dissociation of 2F5 from HIV-1 (data not shown).

To examine whether binding of HIV-1–bNAb ICs to FcγR causes the dissociation of Ab from HIV-1, we transiently transfected HEK 293T cells with FcγRI and assessed capture of HIV-1 treated with 2F5 or b12. There was no discrepancy in the capture of HIV-1 treated with 2F5 or b12, and HIV-1 treated with irrelevant IgG1 gave background capture levels (Fig. 6C). This indicates that both 2F5 and b12 HIV-1–bNAb ICs are intact when captured by FcγRI and do not dissociate after binding, suggesting that another mechanism is used specifically by DCs to cause dissociation of Ab from HIV-1 after capture.

Discussion

Previously, we investigated the neutralization properties of a few earlier-described bNAbs during transfer of HIV-1–Ab complexes

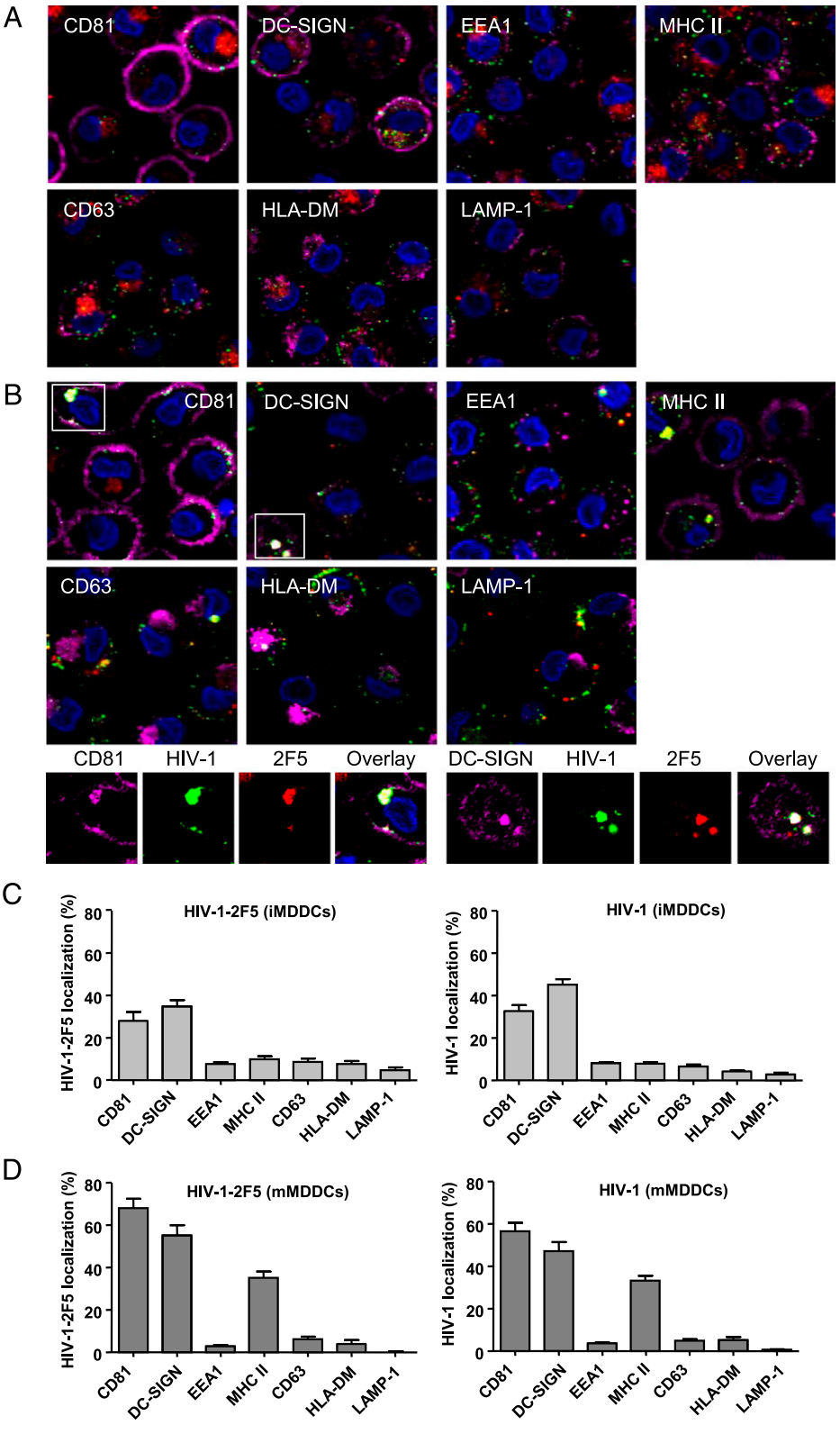

FIGURE 5. Localization of 2F5-neutralized HIV-1 particles in compartments of the endocytic pathway. iMDDCs (**A**) and mMDDCs (**B**) were loaded with 2F5-neutralized HIV-1 particles (HIV-1 in green, Ab in red, nucleus in blue) and stained for the indicated marker proteins: CD81, DC-SIGN, EEA1, MHC class II, CD63, HLA-DM, and LAMP-1 (pink). Cells in (A) and (B) were magnified with a ×64 objective and scanned with a 2× zoom. A zoomed overlay of CD81 or DC-SIGN with HIV-1 and 2F5 bNAb is highlighted in the white boxes and shown underneath (B). (**C** and **D**) Colocalization of intact 2F5–HIV-1 virions (*left panels*) or Ab-free particles (*right panels*) with the indicated compartment marker proteins was calculated as the percentage of total captured virions for iMDDCs and mMDDCs. Data are mean ± SEM from >50 cells.

by iMDDCs (26). In this study, we examined how newly identified potent bNAbs (VRC01, NIH45-46, 10E8, PG9, PG16, PGT121, PGT128, PGT145, PGT151, and 35O22) behaved when Ab-treated HIV-1 was transferred by iDCs or mDCs to HIV-1–susceptible cells. CD4bs bNAbs efficiently blocked HIV-1 transfer by DCs, whereas MPER-directed bNAbs could not. To identify why MPER-directed bNAbs could not block DC-mediated HIV-1 transfer, we studied the processing of HIV-1 complexed with the MPER bNAb 2F5 or CD4bs b12 by iMDDCs and mMDDCs. bNAb 2F5 clustered weakly with HIV-1 in both types of DCs, whereas strong colocalization was observed with b12, reflecting the ability of b12 to inhibit *trans*-infection. No specific compartment of the endocytic pathway was identified as being linked with 2F5 dissociation from virus, leading to the conclusion that dissociation of 2F5 occurred directly at the DC–plasma membrane after HIV-1 capture.

Through the monitoring of multiple MPER-directed and CD4bs bNAbs in the DC-mediated HIV-1 *trans*-infection assay, we demonstrated that the epitope of Env bound by the Ab determined the transfer efficiency. All CD4bs bNAbs efficiently blocked DC-mediated virus transmission, whereas all MPER-directed bNAbs lost their ability to neutralize HIV-1 after capture by DCs and subsequent transmission to HIV-1–susceptible cells. A possible explanation for why MPER bNAbs cannot control HIV-1 neutralization after DC-mediated transfer is their complex binding to their target epitope. In the Env CD4-unliganded prefusion state, both 2F5 and 4E10 first anchor the viral membrane, leading to binding to the MPER, with stronger affinity for the epitope in the CD4-postfusion conformational stage (34, 35). However, the extremely potent 10E8 MPER bNAb is less dependent on binding the viral membrane prior to targeting its epitope (36), but like the other MPER bNAbs, affinity for Env in its prefusion state is weak (37). Thus, it is possible that Ab binding to the MPER in the prefusion state is too weak to withstand HIV-1 processing by DCs. The mechanism for why an MPER bNAb like 2F5 cannot resist DC-mediated HIV-1 transmission was shown for a single R5X4 virus. However, we showed previously that the 2F5 bNAb could not block DC-mediated HIV-1 transmission of viruses using CCR5, CXCR4, or both coreceptors (27). Combined, these results suggest that the MPER Ab-dissociation mechanism is independent of coreceptor usage. Based on the results of this study, it will be interesting to identify whether the other bNAbs behave similarly or differently with viruses representing variant coreceptor phenotypes and how this might correlate with different stages of disease, as well as whether induced Abs can drive virus selection and evolution in infected individuals.

Glycan-dependent bNAbs showed diverse reactions during DC-mediated HIV-1 transfer. PGT121 was the only glycan-dependent bNAb that effectively neutralized HIV-1 when the virus was transferred by iMDDCs or mMDDCs. Shielding of PNGS on Env by bNAbs may well block binding of HIV-1 to C-type lectin receptors on iMDDCs, such as the oligomannose binding receptor DC-SIGN, and thereby reduce *trans*-infection efficiency. The three bNAbs that target the N332 glycan in the outer domain oligomannose patch, 2G12, PGT121, and PGT128 (29), reduced HIV-1 capture by iMDDCs (Fig. 2C), whereas glycan-dependent bNAbs targeting other oligomannose-rich glycans (N160, N230, and N241) did not. Therefore, we speculate that the reduction in HIV-1 capture upon neutralization with 2G12, PGT121, and PGT128 is

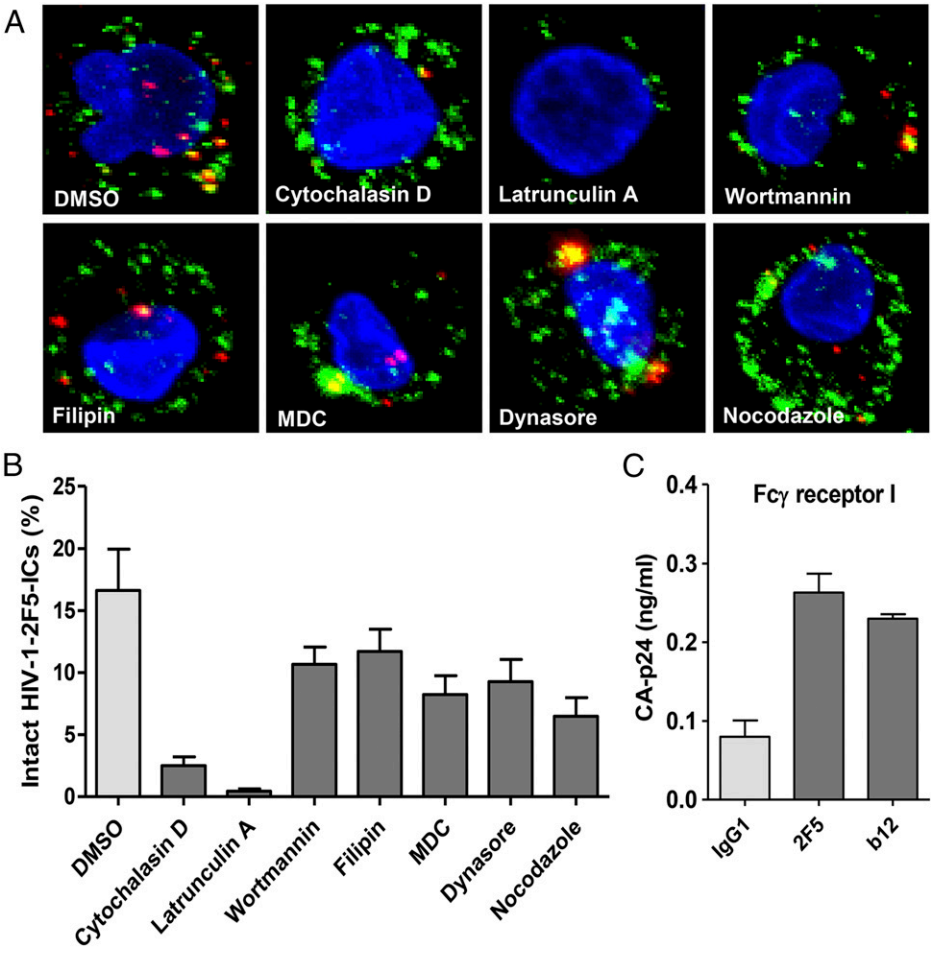

FIGURE 6. Capture of intact HIV-1–Ab ICs by DCs. (**A**) mMDDCs were treated with various compounds that specifically inhibit different internalization pathways and loaded with 2F5-neutralized HIV-1_{GFP} particles (HIV-1 in green, Ab in red, nucleus in blue), and colocalization of 2F5 and HIV-1 was visualized. Cells were magnified with a ×64 objective and scanned with a 2× zoom. (**B**) Colocalization of intact 2F5–HIV-1 particles as the percentage of total captured virions was determined for the different drugs. Data are mean ± SEM from >50 cells. (**C**) Capture of control and 2F5- or b12-neutralized HIV-1 particles by HEK 293T cells expressing FcγRI.

dependent on C-type lectin receptors, such as DC-SIGN. Because mMDDCs predominantly capture HIV-1 by an Env-independent mechanism involving Siglec-1 (i.e., not via C-type lectin receptors), bNAbs that bind Env and inhibit *trans*-infection by iMDDCs have no effect on *trans*-infection by mMDDCs. Interestingly, we could not block the enhanced HIV-1 *trans*-infection observed for PG16 and PGT145 when FcRs were blocked on mMDDCs (data not shown), suggesting that another mechanism or receptor enabled transfer of infectious HIV-1.

Not all glycan-dependent bNAbs were able to neutralize HIV-1 efficiently, although all required the presence of glycans on the R5X4 strain used. Visualization of HIV-1_{GFP} neutralized with the glycan-dependent bNAbs PG9 and PG16 confirmed that bNAb binding indeed occurred (Fig. 3D) without efficiently neutralizing HIV-1. The enhanced transmission of PG16-treated HIV-1 by mMDDCs (Fig. 2A) was not observed with BG505 pseudotyped HIV-1 (Fig. 2B). Instead, PG16 efficiently neutralized BG505, as shown in other reports (38), and neutralized the virus after transfer by iMDDCs or mMDDCs. The difference between Env of the R5X4 strain and BG505 is the sequence of β-strand C in V1V2. BG505 has the amino acid sequence KKQK (LAI numbering 168–171), whereas the R5X4 strain has KGQK. We speculate that the glycans at position N156 and N160 facilitated binding of PG16, whereas virus neutralization also requires efficient Ab binding to β-strand C, as shown by other investigators (30, 31).

The majority of HIV-1 particles was internalized in iMDDCs close to the cell surface. Collecting virus in such loci likely resulted from the formation of invaginations of the plasma membrane, making it unclear whether HIV-1 is inside the cell or remains at the cell surface. mMDDCs sometimes contained large HIV-1 clusters that colocalized with DC-SIGN, CD81, or both, but the majority of HIV-1 was found in small clusters. Uptake of HIV-1 in larger clusters likely occurred via macropinocytosis, a process of nonspecific constitutive engulfment of large volumes of fluid by DCs (39–41). mDCs were shown to collect HIV-1 in a few large clusters containing the tetraspanin CD81 molecule but not in small clusters (16). This result suggests that capture and processing of HIV-1 by mDCs are dependent on the stimulation that is required to trigger DC maturation.

The majority of captured HIV-1 by LPS-matured DCs is Env independent, and binding of HIV-1 occurs via a viral membrane–incorporated ganglioside interaction with the cellular Siglec-1 receptor (23–25). HIV-1 captured by these mDCs end up in a CD81-containing compartment where the virus is protected from degradation. It could be that HIV-1 binding to Siglec-1 is an evolved mechanism that avoids viral degradation (23).

Based on all of our data, we hypothesize three scenarios for 2F5 Ab dissociation from HIV-1. HIV-1 binding to a DC receptor, but not FcγRI (Fig. 6C), induces a conformational change in Env or in the Ab that causes Ab dissociation. Or HIV-1–2F5 ICs are captured Env independently via the membrane binding receptor Siglec-1. Binding of the Siglec-1 receptor or the *trans*-lateral recruitment of the virus to invaginated pockets could mediate Ab dissociation from the virus. Alternatively, the HIV-1–2F5 IC is internalized and enters early transport vesicles of the endosomal pathway, where IgG1-specific FcRn is located (42–44). However, FcRn-blocking experiments did not cause changes in 2F5 dissociation from HIV-1 (data not shown), suggesting that Ab dissociation occurs directly at the plasma membrane.

Our data demonstrate that bNAbs are not always efficient in blocking HIV-1 transmission, but they can show adverse effects in neutralization when transferred by iMDDCs or mMDDCs. It was reported that Abs that bind CD4bs, such as b12, had potent broadly neutralizing activity (45). Combined with the results described in this article, that all CD4bs Abs blocked DC-mediated transmission of HIV-1 to CD4 T cells, the data indicate that future HIV-1 vaccine strategies should aim at inducing such Abs.

Acknowledgments

We thank S. Heynen for performing CA-p24 ELISA assays, T. Hope for providing the GFP-VPR plasmid, and the NIH AIDS Reagent Program (Division of AIDS, National Institute of Allergy and Infectious Diseases) for supplying reagents, bNAbs, and plasmid vectors. We also thank Dr. H. Katinger for the Abs 2F5, 4E10, and 2G12; Dr. D.P. Burton and Dr. P. Parren for b12, PG9, PG16, PGT121, PGT128, and PGT145; Dr. M. Connors for the 10E8 H and L chain expression vectors (35); and Dr. M. Nussenzweig for NIH45-46.

Disclosures

The authors have no financial conflicts of interest.

References

1. Banchereau, J., and R. M. Steinman. 1998. Dendritic cells and the control of immunity. *Nature* 392: 245–252.
2. Banchereau, J., F. Briere, C. Caux, J. Davoust, S. Lebecque, Y. J. Liu, B. Pulendran, and K. Palucka. 2000. Immunobiology of dendritic cells. *Annu. Rev. Immunol.* 18: 767–811.
3. Akira, S., K. Takeda, and T. Kaisho. 2001. Toll-like receptors: critical proteins linking innate and acquired immunity. *Nat. Immunol.* 2: 675–680.
4. Cambi, A., M. Koopman, and C. G. Figdor. 2005. How C-type lectins detect pathogens. *Cell. Microbiol.* 7: 481–488.
5. Figdor, C. G., Y. van Kooyk, and G. J. Adema. 2002. C-type lectin receptors on dendritic cells and Langerhans cells. *Nat. Rev. Immunol.* 2: 77–84.
6. Steinman, R. M., and H. Hemmi. 2006. Dendritic cells: translating innate to adaptive immunity. *Curr. Top. Microbiol. Immunol.* 311: 17–58.
7. Steinman, R. M. 2006. Linking innate to adaptive immunity through dendritic cells. *Novartis Found. Symp.* 279: 101–109, discussion 109–113, 216–219.
8. Turville, S. G., J. J. Santos, I. Frank, P. U. Cameron, J. Wilkinson, M. Miranda-Saksena, J. Dable, H. Stössel, N. Romani, M. Piatak, Jr., et al. 2004. Immunodeficiency virus uptake, turnover, and 2-phase transfer in human dendritic cells. *Blood* 103: 2170–2179.
9. Cavrois, M., J. Neidleman, J. F. Kreisberg, and W. C. Greene. 2007. In vitro derived dendritic cells trans-infect CD4 T cells primarily with surface-bound HIV-1 virions. *PLoS Pathog.* 3: e4.
10. Holl, V., M. Peressin, S. Schmidt, T. Decoville, S. Zolla-Pazner, A. M. Aubertin, and C. Moog. 2006. Efficient inhibition of HIV-1 replication in human immature monocyte-derived dendritic cells by purified anti-HIV-1 IgG without induction of maturation. *Blood* 107: 4466–4474.
11. Geijtenbeek, T. B., D. S. Kwon, R. Torensma, S. J. van Vliet, G. C. van Duijnhoven, J. Middel, I. L. Cornelissen, H. S. Nottet, V. N. KewalRamani, D. R. Littman, et al. 2000. DC-SIGN, a dendritic cell-specific HIV-1-binding protein that enhances trans-infection of T cells. *Cell* 100: 587–597.
12. Arrighi, J. F., M. Pion, E. Garcia, J. M. Escola, Y. van Kooyk, T. B. Geijtenbeek, and V. Piguet. 2004. DC-SIGN-mediated infectious synapse formation enhances X4 HIV-1 transmission from dendritic cells to T cells. *J. Exp. Med.* 200: 1279–1288.
13. Fackler, O. T., A. Alcover, and O. Schwartz. 2007. Modulation of the immunological synapse: a key to HIV-1 pathogenesis? *Nat. Rev. Immunol.* 7: 310–317.
14. McDonald, D., L. Wu, S. M. Bohks, V. N. KewalRamani, D. Unutmaz, and T. J. Hope. 2003. Recruitment of HIV and its receptors to dendritic cell-T cell junctions. *Science* 300: 1295–1297.
15. Thoulouze, M. I., N. Sol-Foulon, F. Blanchet, A. Dautry-Varsat, O. Schwartz, and A. Alcover. 2006. Human immunodeficiency virus type-1 infection impairs the formation of the immunological synapse. *Immunity* 24: 547–561.
16. Garcia, E., M. Pion, A. Pelchen-Matthews, L. Collinson, J. F. Arrighi, G. Blot, F. Leuba, J. M. Escola, N. Demaurex, M. Marsh, and V. Piguet. 2005. HIV-1 trafficking to the dendritic cell-T-cell infectious synapse uses a pathway of tetraspanin sorting to the immunological synapse. *Traffic* 6: 488–501.
17. Izquierdo-Useros, N., M. Naranjo-Gómez, J. Archer, S. C. Hatch, I. Erkizia, J. Blanco, F. E. Borràs, M. C. Puertas, J. H. Connor, M. T. Fernández-Figueras, et al. 2009. Capture and transfer of HIV-1 particles by mature dendritic cells converges with the exosome-dissemination pathway. *Blood* 113: 2732–2741.
18. Wu, L., T. D. Martin, Y. C. Han, S. K. Breun, and V. N. KewalRamani. 2004. Trans-dominant cellular inhibition of DC-SIGN-mediated HIV-1 transmission. *Retrovirology* 1: 14.
19. Akiyama, H., N.-G. P. Ramirez, M. V. Gudheti, and S. Gummuluru. 2015. CD169-mediated trafficking of HIV to plasma membrane invaginations in dendritic cells attenuates efficacy of anti-gp120 broadly neutralizing antibodies. [Published erratum appears in 2015 *PLoS Pathog.*11: e1004751. Available at: http://journals.plos.org/plospathogens/article?id=10.1371/journal.ppat.1004751.
20. Roderiquez, G., T. Oravecz, M. Yanagishita, D. C. Bou-Habib, H. Mostowski, and M. A. Norcross. 1995. Mediation of human immunodeficiency virus type 1 binding by interaction of cell surface heparan sulfate proteoglycans with the V3 region of envelope gp120-gp41. *J. Virol.* 69: 2233–2239.

21. Bobardt, M. D., A. C. Saphire, H. C. Hung, X. Yu, B. Van der Schueren, Z. Zhang, G. David, and P. A. Gallay. 2003. Syndecan captures, protects, and transmits HIV to T lymphocytes. *Immunity* 18: 27–39.
22. de Witte, L., M. Bobardt, U. Chatterji, G. Degeest, G. David, T. B. Geijtenbeek, and P. Gallay. 2007. Syndecan-3 is a dendritic cell-specific attachment receptor for HIV-1. *Proc. Natl. Acad. Sci. USA* 104: 19464–19469.
23. Izquierdo-Useros, N., M. Lorizate, M. C. Puertas, M. T. Rodriguez-Plata, N. Zangger, E. Erikson, M. Pino, I. Erkizia, B. Glass, B. Clotet, et al. 2012. Siglec-1 is a novel dendritic cell receptor that mediates HIV-1 trans-infection through recognition of viral membrane gangliosides. *PLoS Biol.* 10: e1001448.
24. Puryear, W. B., X. Yu, N. P. Ramirez, B. M. Reinhard, and S. Gummuluru. 2012. HIV-1 incorporation of host-cell-derived glycosphingolipid GM3 allows for capture by mature dendritic cells. *Proc. Natl. Acad. Sci. USA* 109: 7475–7480.
25. Puryear, W. B., H. Akiyama, S. D. Geer, N. P. Ramirez, X. Yu, B. M. Reinhard, and S. Gummuluru. 2013. Interferon-inducible mechanism of dendritic cell-mediated HIV-1 dissemination is dependent on Siglec-1/CD169. *PLoS Pathog.* 9: e1003291.
26. van Montfort, T., A. A. Nabatov, T. B. Geijtenbeek, G. Pollakis, and W. A. Paxton. 2007. Efficient capture of antibody neutralized HIV-1 by cells expressing DC-SIGN and transfer to CD4+ T lymphocytes. *J. Immunol.* 178: 3177–3185.
27. van Montfort, T., A. A. Thomas, G. Pollakis, and W. A. Paxton. 2008. Dendritic cells preferentially transfer CXCR4-using human immunodeficiency virus type 1 variants to CD4+ T lymphocytes in trans. *J. Virol.* 82: 7886–7896.
28. Pollakis, G., S. Kang, A. Kliphuis, M. I. Chalaby, J. Goudsmit, and W. A. Paxton. 2001. N-linked glycosylation of the HIV type-1 gp120 envelope glycoprotein as a major determinant of CCR5 and CXCR4 coreceptor utilization. *J. Biol. Chem.* 276: 13433–13441.
29. Pritchard, L. K., D. I. R. Spencer, L. Royle, C. Bonomelli, G. E. Seabright, A.-J. Behrens, D. W. Kulp, S. Menis, S. A. Krumm, D. C. Dunlop, et al. 2015. Glycan clustering stabilizes the mannose patch of HIV-1 and preserves vulnerability to broadly neutralizing antibodies. *Nat. Commun.* DOI: 10.1038/ncomms8479.
30. McLellan, J. S., M. Pancera, C. Carrico, J. Gorman, J. P. Julien, R. Khayat, R. Louder, R. Pejchal, M. Sastry, K. Dai, et al. 2011. Structure of HIV-1 gp120 V1/V2 domain with broadly neutralizing antibody PG9. *Nature* 480: 336–343.
31. Ringe, R., S. Phogat, and J. Bhattacharya. 2012. Subtle alteration of residues including N-linked glycans in V2 loop modulate HIV-1 neutralization by PG9 and PG16 monoclonal antibodies. *Virology* 426: 34–41.
32. Schuurhuis, D. H., A. Ioan-Facsinay, B. Nagelkerken, J. J. van Schip, C. Sedlik, C. J. Melief, J. S. Verbeek, and F. Ossendorp. 2002. Antigen-antibody immune complexes empower dendritic cells to efficiently prime specific CD8+ CTL responses in vivo. *J. Immunol.* 168: 2240–2246.
33. Davies, P. J., D. R. Davies, A. Levitzki, F. R. Maxfield, P. Milhaud, M. C. Willingham, and I. H. Pastan. 1980. Transglutaminase is essential in receptor-mediated endocytosis of alpha 2-macroglobulin and polypeptide hormones. *Nature* 283: 162–167.
34. Alam, S. M., M. Morelli, S. M. Dennison, H. X. Liao, R. Zhang, S. M. Xia, S. Rits-Volloch, L. Sun, S. C. Harrison, B. F. Haynes, and B. Chen. 2009. Role of HIV membrane in neutralization by two broadly neutralizing antibodies. *Proc. Natl. Acad. Sci. USA* 106: 20234–20239.
35. Sun, Z. Y., K. J. Oh, M. Kim, J. Yu, V. Brusic, L. Song, Z. Qiao, J. H. Wang, G. Wagner, and E. L. Reinherz. 2008. HIV-1 broadly neutralizing antibody extracts its epitope from a kinked gp41 ectodomain region on the viral membrane. *Immunity* 28: 52–63.
36. Huang, J., G. Ofek, L. Laub, M. K. Louder, N. A. Doria-Rose, N. S. Longo, H. Imamichi, R. T. Bailer, B. Chakrabarti, S. K. Sharma, et al. 2012. Broad and potent neutralization of HIV-1 by a gp41-specific human antibody. *Nature* 491: 406–412.
37. Chen, J., G. Frey, H. Peng, S. Rits-Volloch, J. Garrity, M. S. Seaman, and B. Chen. 2014. Mechanism of HIV-1 neutralization by antibodies targeting a membrane-proximal region of gp41. *J. Virol.* 88: 1249–1258.
38. Sanders, R. W., R. Derking, A. Cupo, J. P. Julien, A. Yasmeen, N. de Val, H. J. Kim, C. Blattner, A. T. de la Peña, J. Korzun, et al. 2013. A next-generation cleaved, soluble HIV-1 Env trimer, BG505 SOSIP.664 gp140, expresses multiple epitopes for broadly neutralizing but not non-neutralizing antibodies. *PLoS Pathog.* 9: e1003618.
39. Frank, I., M. Piatak, Jr., H. Stoessel, N. Romani, D. Bonnyay, J. D. Lifson, and M. Pope. 2002. Infectious and whole inactivated simian immunodeficiency viruses interact similarly with primate dendritic cells (DCs): differential intracellular fate of virions in mature and immature DCs. *J. Virol.* 76: 2936–2951.
40. Maréchal, V., M. C. Prevost, C. Petit, E. Perret, J. M. Heard, and O. Schwartz. 2001. Human immunodeficiency virus type 1 entry into macrophages mediated by macropinocytosis. *J. Virol.* 75: 11166–11177.
41. Wang, J. H., C. Wells, and L. Wu. 2008. Macropinocytosis and cytoskeleton contribute to dendritic cell-mediated HIV-1 transmission to CD4+ T cells. *Virology* 381: 143–154.
42. Ghetie, V., and E. S. Ward. 2000. Multiple roles for the major histocompatibility complex class I- related receptor FcRn. *Annu. Rev. Immunol.* 18: 739–766.
43. Popov, S., J. G. Hubbard, J. Kim, B. Ober, V. Ghetie, and E. S. Ward. 1996. The stoichiometry and affinity of the interaction of murine Fc fragments with the MHC class I-related receptor, FcRn. *Mol. Immunol.* 33: 521–530.
44. Raghavan, M., V. R. Bonagura, S. L. Morrison, and P. J. Bjorkman. 1995. Analysis of the pH dependence of the neonatal Fc receptor/immunoglobulin G interaction using antibody and receptor variants. *Biochemistry* 34: 14649–14657.
45. Li, Y., S. A. Migueles, B. Welcher, K. Svehla, A. Phogat, M. K. Louder, X. Wu, G. M. Shaw, M. Connors, R. T. Wyatt, and J. R. Mascola. 2007. Broad HIV-1 neutralization mediated by CD4-binding site antibodies. *Nat. Med.* 13: 1032–1034.
46. Walker, L. M., S. K. Phogat, P. Y. Chan-Hui, D. Wagner, P. Phung, J. L. Goss, T. Wrin, M. D. Simek, S. Fling, J. L. Mitcham, et al; Protocol G Principal Investigators. 2009. Broad and potent neutralizing antibodies from an African donor reveal a new HIV-1 vaccine target. *Science* 326: 285–289.
47. Pancera, M., S. Shahzad-Ul-Hussan, N. A. Doria-Rose, J. S. McLellan, R. T. Bailer, K. Dai, S. Loesgen, M. K. Louder, R. P. Staupe, Y. Yang, et al. 2013. Structural basis for diverse N-glycan recognition by HIV-1-neutralizing V1-V2-directed antibody PG16. *Nat. Struct. Mol. Biol.* 20: 804–813.
48. Sanders, R. W., M. Venturi, L. Schiffner, R. Kalyanaraman, H. Katinger, K. O. Lloyd, P. D. Kwong, and J. P. Moore. 2002. The mannose-dependent epitope for neutralizing antibody 2G12 on human immunodeficiency virus type 1 glycoprotein gp120. *J. Virol.* 76: 7293–7305.
49. Scanlan, C. N., R. Pantophlet, M. R. Wormald, E. Ollmann Saphire, R. Stanfield, I. A. Wilson, H. Katinger, R. A. Dwek, P. M. Rudd, and D. R. Burton. 2002. The broadly neutralizing anti-human immunodeficiency virus type 1 antibody 2G12 recognizes a cluster of alpha1→2 mannose residues on the outer face of gp120. *J. Virol.* 76: 7306–7321.
50. Mouquet, H., L. Scharf, Z. Euler, Y. Liu, C. Eden, J. F. Scheid, A. Halper-Stromberg, P. N. Gnanapragasam, D. I. Spencer, M. S. Seaman, et al. 2012. Complex-type N-glycan recognition by potent broadly neutralizing HIV antibodies. *Proc. Natl. Acad. Sci. USA* 109: E3268–E3277.
51. Walker, L. M., M. Huber, K. J. Doores, E. Falkowska, R. Pejchal, J. P. Julien, S. K. Wang, A. Ramos, P. Y. Chan-Hui, M. Moyle, et al; Protocol G Principal Investigators. 2011. Broad neutralization coverage of HIV by multiple highly potent antibodies. *Nature* 477: 466–470.
52. Sok, D., K. J. Doores, B. Briney, K. M. Le, K. L. Saye-Francisco, A. Ramos, D. W. Kulp, J. P. Julien, S. Menis, L. Wickramasinghe, et al. 2014. Promiscuous glycan site recognition by antibodies to the high-mannose patch of gp120 broadens neutralization of HIV. *Sci. Transl. Med.* 6: 236ra63.
53. Pejchal, R., K. J. Doores, L. M. Walker, R. Khayat, P. S. Huang, S. K. Wang, R. L. Stanfield, J. P. Julien, A. Ramos, M. Crispin, et al. 2011. A potent and broad neutralizing antibody recognizes and penetrates the HIV glycan shield. *Science* 334: 1097–1103.
54. Kong, L., J. H. Lee, K. J. Doores, C. D. Murin, J. P. Julien, R. McBride, Y. Liu, A. Marozsan, A. Cupo, P. J. Klasse, et al. 2013. Supersite of immune vulnerability on the glycosylated face of HIV-1 envelope glycoprotein gp120. *Nat. Struct. Mol. Biol.* 20: 796–803.
55. Blattner, C., J. H. Lee, K. Sliepen, R. Derking, E. Falkowska, A. T. de la Peña, A. Cupo, J. P. Julien, M. van Gils, P. S. Lee, et al. 2014. Structural delineation of a quaternary, cleavage-dependent epitope at the gp41-gp120 interface on intact HIV-1 Env trimers. *Immunity* 40: 669–680.
56. Falkowska, E., K. M. Le, A. Ramos, K. J. Doores, J. H. Lee, C. Blattner, A. Ramirez, R. Derking, M. J. van Gils, C. H. Liang, et al. 2014. Broadly neutralizing HIV antibodies define a glycan-dependent epitope on the prefusion conformation of gp41 on cleaved envelope trimers. *Immunity* 40: 657–668.
57. Huang, J., B. H. Kang, M. Pancera, J. H. Lee, T. Tong, Y. Feng, H. Imamichi, I. S. Georgiev, G. Y. Chuang, A. Druz, et al. 2014. Broad and potent HIV-1 neutralization by a human antibody that binds the gp41-gp120 interface. *Nature* 515: 138–142.
58. Pancera, M., T. Zhou, A. Druz, I. S. Georgiev, C. Soto, J. Gorman, J. Huang, P. Acharya, G. Y. Chuang, G. Ofek, et al. 2014. Structure and immune recognition of trimeric pre-fusion HIV-1 Env. *Nature* 514: 455–461.